Identifying the controls on nitrate and metabolic state within the Red River delta (Vietnam) with the use of stable isotopes

Authors: Andrew Smith[1], Melanie Leng[1], Suzanne McGowan[2], Virginia N Panizzo[3], Ngo Thi Thu Trang[4], Luu Thi Nguyet Minh[4], Ioannis Matiatos[5], Do Thu Nga[6], Ta Thi Thao[7], Trinh Anh Duc[8*]

[1] British Geological Survey, Nottingham, NG12 5GG, UK.

[2] Department of Aquatic Ecology, Netherlands Institute of Ecology, Droevendaalsesteeg 10, 6708PB, Wageningen, The Netherlands. Orcid: 0000-0003-4034-7140

[3] Centre for Environmental Geochemistry, School of Geography, University of Nottingham, University Park, Nottingham NG7 2RD, United Kingdom

[4] Institute of Chemistry, Vietnam Academy of Science and Technology, A18, 18 Hoang Quoc Viet, Cau Giay, Ha Noi, Viet Nam

[5] Hellenic Centre for Marine Research, Institute of Marine Biological Resources and Inland Waters, 19013 Anavissos Attikis, Greece

[6] Faculty of Energy Technology, Electric Power University (EPU), 235 Hoang Quoc Viet, Cau Giay, Ha Noi 11900, Viet Nam; dothu_nga2005@yahoo.com

[7] Faculty of Chemistry, University of Natural Sciences, Hanoi National University, 19 Le Thanh Tong, Hoan Kiem, Ha Noi, Viet Nam

[8] Nuclear Training Center, Vietnam Atomic Energy Institute, 140 Nguyen Tuan, Thanh Xuan, Ha Noi, Viet Nam; trinhanhduc@vinatom.gov.vn. Orcid: 0000-0003-4207-8845

Abstract:

In many places around the world, anthropogenic activities have resulted in nitrate (NO_3^-) pollution and changes in the metabolic state of aquatic ecosystems. Here we combined stable isotope and physico-chemical monitoring to assess the sources of NO_3^- and the overall metabolic state within the Red River delta, Vietnam. River water stable isotope compositions ($\delta^{18}O\text{-}H_2O$) ranged between -11.2 and -2.7 ‰, $\delta^{18}O\text{-}NO_3^-$ between -7.1 and +29.7 ‰ and $\delta^{15}N\text{-}NO_3^-$ between -3.9 and +14.0 ‰. We identified the dominant NO_3^- sources as: 1) soil leachate, 2) domestic waste flushed from urban areas, and 3) NH_4^+ fertilizers washed from paddy fields. The relative impact of each source depends on geographical location within the delta and the time of year, due to dilution and concentration effects during wet and dry seasons. The primary NO_3^-source upstream is natural soil leachates, predominantly from tributaries connected to the Red River's main stream. Within the middle-lower section of Red River delta, urban pollution from manure and septic waste reaches as high as 50 % of the total NO_3^- load during dry season. NO_3^- leached from fertilizers is also high at sites in the middle of the delta, related to agricultural activities. Dissolved oxygen isotope ($\delta^{18}O\text{-}O_2$) values calculated from $\delta^{18}O\text{-}H_2O$ and $\delta^{18}O\text{-}NO_3^-$ values indicate that the aquatic metabolism is net autotrophic (oxygen from primary production exceeds consumption by respiration), but high inputs of biodegradable organic matter from untreated domestic waste and high rates of sediment oxygen demand (SOD) and chemical oxygen demand (COD) have resulted in the whole river system becoming undersaturated in oxygen. High NO_3^- loads and low DO saturation are of critical concern and require mitigation practices to improve water quality for millions of people.

Keywords: Water stable isotopes, dual NO_3^- stable isotopes, nitrification, denitrification, dissolved oxygen isotope, aquatic metabolism

Highlights:

- NO_3^- is formed from nitrification of soil leachate, domestic waste, and NH_4^+ fertilizers
- Denitrification occurs at heavily impacted domestic waste sites
- The Red River is autotrophic, despite being undersaturated in dissolved oxygen
- Manure and septic waste contribute 50 % of NO_3^- in the middle-lower section during the dry period
- High loading of fertilizer-leached NO_3^- is driven by agricultural activities

Introduction

Many of the world's largest river systems are becoming significantly impacted by anthropogenic activities, including, importantly, the pollution of these systems by key nutrients (Strokal, et al., 2016; Steffen, et al., 2015). Nutrients discharged from human activities such as industry, agriculture and urban settlements (often wastewater) can overload these once pristine systems, leading to environmental degradation, eutrophication and ecosystem collapse (Trinh, et al., 2007; Salgado, et al., 2022). Alongside the environmental issues such pollutants cause, these waters become unsafe for human consumption, or for further use downstream of the pollutant source (Zeng, et al., 2023). These issues are now global in nature and have led to widespread efforts to understand the sources of pollution and the mechanisms of nutrient addition, processing, and removal, occurring in anthropogenically impacted river systems (Steffen, et al.,

63 2015). Only through a wide reaching spatial and temporal understanding of nutrient dynamics
64 within any river system can effective mitigation strategies be implemented (Xue, et al., 2009;
65 Matiatos, et al., 2021; Matiatos, et al., 2023).

66 One of the key nutrients of interest for many impacted systems is nitrogen (N). N is often
67 considered a limiting nutrient within aquatic systems under natural conditions (Denk, et al.,
68 2017). Most rivers have natural sources of N delivered in limited abouts via atmospheric
69 deposition often as nitrate (NO_3^-), groundwater inflow (Marković, et al., 2022), biological N
70 fixation (Denk, et al., 2017), upstream soil leaching, or particulate soil inputs from erosion and
71 flooding events. Additionally, NO_3^- and ammonia (NH_3) can enter rivers because of uncontrolled
72 human waste disposal, industrial activities or direct leaching from fertilizers applied to
73 agricultural systems (Venkiteswaran, et al., 2019). When there is a significant input of N through
74 anthropogenic activities, N is no longer a limiting nutrient, and the system can rapidly become
75 eutrophic.

76 Nitrogen and oxygen stable isotope composition of NO_3^- ($\delta^{15}N$ and $\delta^{18}O$) have been used as
77 reliable tracers (Denk, et al., 2017) for the sources and transformation processes of N such as for
78 the conversion of NH_4^+ to NO_3^- via nitrification. Using this dual isotope methodology, numerous
79 studies have assessed the origin of nitrate pollution (Kendall, 1998) and isotopic fractionations
80 can be associated with processes, such as nitrification and denitrification (Pardo, et al., 2004). In
81 well studied systems we can therefore use these isotope tracers to obtain information about the
82 sources and fates of N (Matiatos, et al., 2021). In addition, in an aquatic ecosystem dominated
83 by nitrification, the nitrate oxygen isotope (^{18}O of nitrate) in combination with the water oxygen
84 isotope (^{18}O of H_2O) can be used to calculate the dissolved oxygen isotope value. This oxygen

isotope value can in turn be used to assess the aquatic metabolism (Venkiteswaran, et al., 2007; Piatka, et al., 2022). Here we apply nitrate isotopes and water isotopes to 1) assess the NO_3^- sources and identify the processes governing NO_3^- within stream water and 2) assess aquatic ecosystem metabolism within the Red River delta, which supports two of Vietnam's largest rivers, the Red River and the Day River (a significant tributary located in the heart of urban Vietnam) (Luu, et al., 2020).

Site description and methods

Description of the Red River delta and its river network

The Red River is over 1000 km in length, and its source originates in China before flowing through densely populated regions within Vietnam and terminating in the Red River delta- gulf of Tonkin. The Red River delta is the most populous area in Vietnam, concentrated with agricultural (rice paddy farming) and industrial activities, as well as housing high density urban areas including Hanoi (Trinh, et al., 2007). The diversity of activities within the Red River region means there are several potential sources of NO_3^- in the Red River delta. These include NO_3^- derived from largely natural upstream sources (Luu, et al., 2020), soil derived from within the delta, inorganic fertilizers used in rice agriculture, industrial/urban outwash and domestic waste (Roberts, et al., 2022).

Industrial-related activities within the catchment have impacted the natural river system. Deviations of the river's natural course to facilitate urban water use, improve transport and feed agricultural practices mean that many parts of the tributary network are no longer connected to the main stream. Such parts (e.g., the upper part of Day River) are now heavily managed and

106 serve different water resource purposes. The Day River used to be naturally connected to the
107 Red River mainstream at several locations, but in order to function as the drainage system for
108 the Hanoi metropolitan district and its surrounding populations, the upper section has been
109 virtually cut off from the Red River. The Day River is disconnected from the larger Red River
110 system and only collects water from its own catchment. The Day River catchment houses more
111 than 10 million people and is regionally critical for agriculture and industry. The high demands on
112 this water resource and its managed connection to the Red River have, in combination, resulted
113 in significant degradation in water quality in recent years (Trinh, et al., 2007).

114 Monitoring sites are located in the Red River main stream receiving water from upstream
115 mountains and its tributary, the Day River, in the Red River delta (Table 1, Fig. 1).

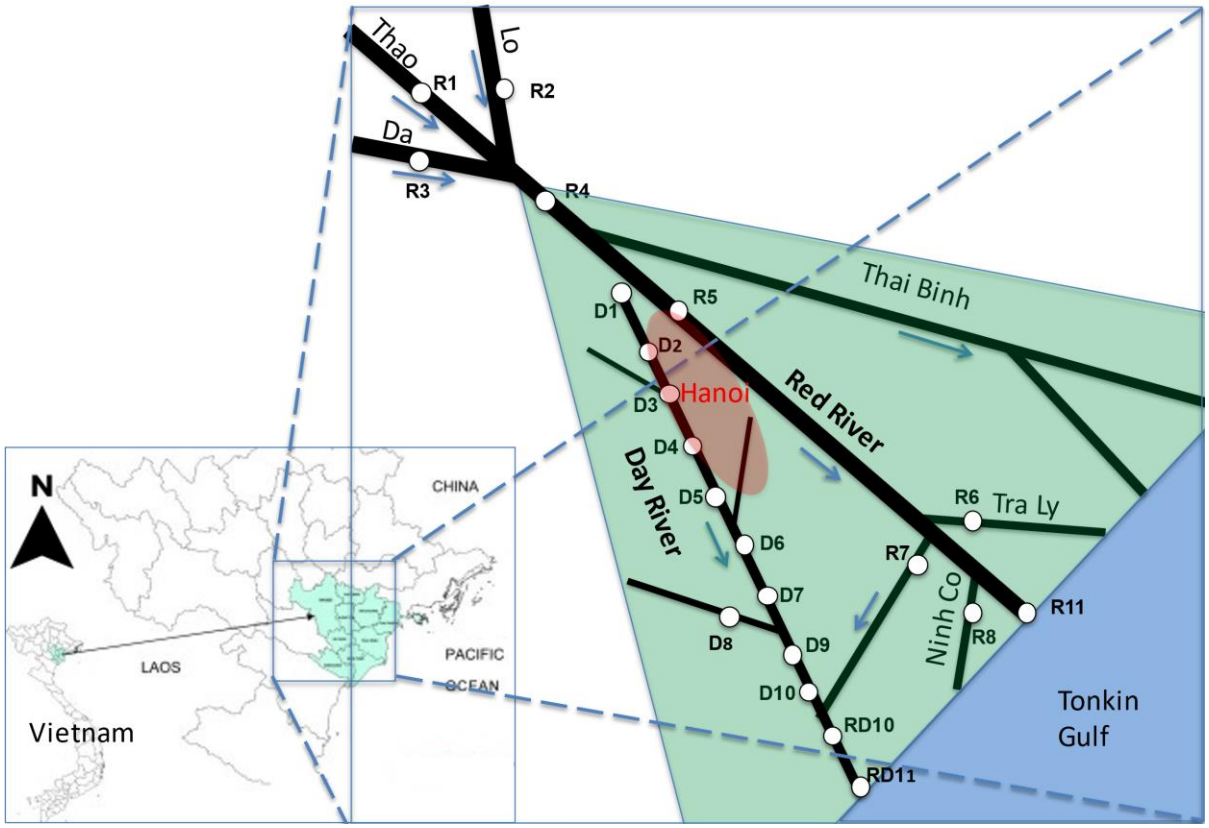

Fig. 1: Schematic of the main water ways in the Red River delta (the monitoring part) and sampling sites; Hanoi is an urban area. For other parts in the delta, the urban, industrial, and agricultural activities are intertwined. The figure is not in spatial scale.

Table 1: Names and locations of the sampling sites (Specific locations are in Fig. 1). Sites prefixed with R receive water from both upstream mountain and delta region and the D group receive water from inside delta region only.

Site name	River reach	Longitude (°E)	Latitude (°N)	Altitude (m)
Yen Bai (R1)	Thao River, upstream central	104.88333	21.70000	60
Vu Quang (R2)	Lo River, upstream left	105.25000	21.56667	22
Hoa Binh (R3)	Da River, upstream right	105.31667	20.81667	120
Son Tay (R4)	Red River	105.43700	21.22700	15

Ha Noi (R5)	Red River, delta	105.85000	21.03333	10
Quyet Chien (R6)	Tra Ly River, delta	106.25000	20.50000	2
Nam Dinh (R7)	Dao River, delta	106.16667	20.41667	2
Truc Phuong (R8)	Ninh Co River, delta	106.26667	20.31667	2
Do Muoi (RD10)	Red+Day River	106.16600	20.14200	1
Cua Day (RD11)	Red+Day River, estuarine zone	106.10300	19.92800	0
Ba Lat (R11)	Red River, estuarine zone	106.52600	20.32100	0
Phung (D1)	Day River	105.64513	21.07521	12
Mai Linh (D2)	Day River	105.72711	20.93646	11
Ba Tha (D3)	Day River	105.70722	20.80583	10
Te Tieu (D4)	Day River	105.74710	20.68646	9
Que (D5)	Day River	105.87263	20.57451	8
Do (D6)	Day River	105.91151	20.51578	7
Doan Vi (D7)	Day River	105.92081	20.36240	3
Gian Khau (D8)	Day River	105.91667	20.31667	3
Non Nuoc (D9)	Day River	105.98071	20.26526	3
Do Thong (D10)	Day River	106.04511	20.21738	2

Sampling and *in situ* measurements

River water samples were collected during 10 different sampling campaigns between October 2016 and February 2022. Samples were collected at a distance of approx. 10 m from the river's bank and divided into sub-samples for analysis of nitrogen (N) concentrations and stable isotope analyses (water and nitrate). For water stable isotope analyses ($\delta^{18}O$ and $\delta^{2}H$ of H_2O), the sub-samples were filtered in the field with Sartorius technical filter papers (8 μm pore size) and collected in 30 ml HDPE plastic bottles. They were then kept at 20°C with no headspace in the bottle prior to analysis at the Isotope Hydrology Laboratory of the International Atomic Energy Agency (IAEA), Vienna, Austria. Physico-chemical parameters including dissolved oxygen (DO) were monitored *in situ* using a Hydrolab Sonde DS5.

Dissolved nitrogen analysis

The analytical procedures for dissolved nitrogen compounds were conducted in the Institute of Chemistry (ICH), Vietnam Academy of Science and Technology (VAST), in accordance with the Standard Methods for the Examination of Water and Wastewater (Clesceri, et al., 1998). The 1 L sub-samples were kept below 4^{o}C to prevent significant degradation during storage and analyzed within 48 hours. Nitrate was determined by quantitative reduction to nitrite on a cadmium column, followed by colorimetric determination at 540 nm of nitrite using the Griess reaction (Standard method 4500-NO3 E in (Clesceri, et al., 1998). The detection limit (DL) of the NO_3^- analysis was 0.02 mg NO_3^- L^{-1}.

Water stable isotope analysis

All samples were pipetted into 2 mL laser vials and measured using a high-precision Los Gatos Research liquid water isotope analyzer model 912-0032 (Los Gatos Research (www.lgrinc.com, California, USA)). The method consisted of 9 injections per vial, ignoring the first 4 to eliminate memory effect, with data processing procedures to correct for between-sample memory and instrumental drift, and normalization to the VSMOW-SLAP scale using LIMS for Lasers 2015 as fully described elsewhere (Wassenaar, et al., 2014; Coplen & Wassenaar, 2015). A 2-point normalization was applied using IAEA laboratory standards W-34 (low standard) and W-39 (high standard) to bracket the isotopic composition of the samples. IAEA laboratory standards were calibrated using VSMOW2 and SLAP2 primary reference materials. The assigned $\delta^{18}O$ and $\delta^{2}H$ values for the laboratory calibration standards were W-39 (+3.6±0.04 ‰ and +25.4±0.8 ‰), W-34 (-24.8±0.02 ‰ and -189.5±0.9 ‰) and control W-31 (-8.6±0.09 ‰ and 61.0±0.6 ‰), relative

to VSMOW, respectively. The control W-31 long-term (1-yr running average) analytical reproducibility (±SD) was ±0.11 ‰ and ±0.7 ‰ for $\delta^{18}O$ and $\delta^{2}H$, respectively.

Dual nitrogen stable isotope analysis

Prior to July 2019, the water samples for dual stable isotope analysis of NO_3^- were filtered with GF/F Whatman filters, stored in acid-cleaned, high-density polyethylene (HDPE) bottles and frozen prior shipment to the Isotope Hydrology Laboratory of IAEA for analysis. The Cd-azide reduction method to headspace N_2O gas was used as fully described in McIlvin & Altabet (2005). The instrument used was an Isoprime 100 with a Trace Gas (TG) system linked to a continuous flow isotope ratio mass spectrometer (CF-IRMS) system (Isoprime Ltd, Cheadle Hulme, UK). The Isoprime CF-IRMS system operated at an external analytical precision of ±0.2 ‰ ($\delta^{15}N$-N_2O values) and ±0.3 ‰ ($\delta^{18}O$-N_2O values) using 2-point normalization using dissolved nitrate reference materials (USGS32, USGS34, USGS35, IAEA NO3).

The last two batches of samples (July 2019 and February 2020) were treated and analyzed at the British Geological Survey (BGS), UK following the ionex method (Chang, et al., 1999; Silva, et al., 2000). Ten liters of sample were passed through two conditioned ion exchange columns, firstly a cation resin column and then an anion resin for NO_3^- capture. NO_3^- was eluted from the anion resin using 25ml of HBr, captured and 2.5-3 g of washed Ag_2O added on a magnetic stirrer until pH 6-7 was reached. The solution was filtered through a 0.2 µm polycarbonate filter before 4ml of 1M $BaCl_2$ was added and left overnight to precipitate. The solution was then passed through a Dowex 50WX8 cation resin to remove excess barium. This solution had a further 1 g of Ag_2O added until a pH of 6 was reached, the samples were filtered before freezing overnight. The

frozen samples were freeze dried and the resultant NO_3^- solids were re-dissolved in 1ml of MilliQ H_2O before being centrifuged and ready for analysis with the mass spectrometry. The $\delta^{18}O\text{-}NO_3^-$ analysis was conducted on a TC pyrolysis elemental analyser (EA) coupled to a Thermo Fisher Delta XL Isotope Ratio Mass Spectrometer (IRMS). Nitrogen isotope analysis of silver nitrate ($\delta^{15}N\text{-}NO_3^-$) was undertaken on a Flash elemental analyser (EA) coupled to a Thermo Fisher Delta XL Isotope Ratio Mass Spectrometer (IRMS). External reference materials: IAEA-N1, IAEA N2 and IAEA-NO_3 for $\delta\,^{15}N\text{-}NO_3^-$ and USGS 32, 34 and 35 and IAEA-NO_3 for $\delta\,^{18}O\text{-}NO_3^-$ were treated the same way as the samples. Oxygen isotope values were corrected to the international VSMOW scale and nitrogen to AIR. Typical precision is <1.5 ‰ for $\delta^{18}O\text{-}NO_3^-$ and <0.3 ‰ for $\delta^{15}N\text{-}NO_3^-$ based on within run replication of reference materials.

Mixing model formulation

We assumed the following three main sources of nitrate based on the geographical and natural conditions of the Red River delta (e.g., (Ta, et al., 2016; Luu, et al., 2020): (1) inputs from soil and groundwater sources (natural, background input levels), (2) inputs from regional, excessive application rates of chemical fertilizers (NH_4^+), and (3) inputs from organic matter deriving from urban regions and livestock farming (sewage and manure). In order to derive the proportions of these sources, we used the following partition equations of NO_3^-, which are based on our stable isotope data:

$$\delta^{18}O = f_S\delta^{18}O_S + f_P\delta^{18}O_P + f_M\delta^{18}O_M \quad (1)$$

$$\delta^{15}N = f_S\delta^{15}N_S + f_P\delta^{15}N_P + f_M\delta^{15}N_M \quad (2)$$

$$1 = f_S + f_P + f_M \quad (3)$$

Of which f_S, f_P, and f_M are respectively the partition coefficients of each of the 3 main sources described above: 1) soil and groundwater input, 2) NH_4^+ fertilization run off from paddy fields and 3) sewage and manure discharge.

We utilised source values either derived from this study or from Luu et al., (2020) (Table 2), to enable a spatial assessment of the changing source apportionment throughout the Red and Day River catchments. We used averaged $\delta^{15}N\text{-}NO_3^-$ and $\delta^{18}O\text{-}NO_3^-$ at R2 as a representative soil source end member, as water at this site derives from a largely natural mountain catchment. $\delta^{15}N$ end members for NH_4^+ fertilizer and urban waste sources are taken from (Luu, et al., 2020). The $\delta^{18}O$ values assigned to these sources are produced in this study, supplemented by data from (Luu, et al., 2020) where necessary (Table 2).

Table 2: End member compositions of $\delta^{18}O$ and $\delta^{15}N$ of nitrate used in this study for the partition calculations.

	Soil		Fertilizer		Urban	
	$\delta^{15}N\text{-}NO_3^-$	$\delta^{18}O\text{-}NO_3^-$	$\delta^{15}N\text{-}NO_3^-$	$\delta^{18}O\text{-}NO_3^-$	$\delta^{15}N\text{-}NO_3^-$	$\delta^{18}O\text{-}NO_3^-$
Day River	+4.5 – 7.9[(a)]	+0.7 – 7.8[(a,b)]	-5.9[(a)]	-12.3 – -5.7[(a,b)]	+16.2[(a)]	-4.4 – 0.6[(a,b)]
Red River	+4.5 – 7.9[(a)]	+2.1 – 2.6[(b)]	-5.9[(a)]	-10.1 – -7.9[(b)]	+16.2[(a)]	-5.7 – -5.2[(b)]

Sources/pools are defined constantly for $\delta^{15}N\text{-}NO_3^-$ and vary seasonally for $\delta^{18}O\text{-}NO_3^-$ data derived from either (a) (Luu, et al., 2020) or (b) this study.

Results and discussion

Sources of water in the Red River delta

The dissolved oxygen concentration ranged between 1.65±1.25 mg L^{-1} at point D2 and 5.62±1.2 mg L^{-1}) at point R7 (Fig. 1, Appendix). In general, DO was low (< 3.5 mg L^{-1}) in the D group sites and high (> 4 mg L^{-1}) in the R group sites.

Water stable isotope values indicate two distinct water sources within the Red River delta (Fig. 2a). The first consists of sites R1-8, and RD10 (Red River group), which are fed by upstream waters delivered from the mountainous region of Yunan Province (China) and the north and northwestern mountains of Vietnam (Fig. 1). These sites are characterised by lower water $\delta^{18}O$ (-11.7 to -6.5 ‰) and $\delta^{2}H$ (-85 to -45 ‰) values than the second group (Day River group, sites D1-10), which only drains water from inside the delta ($\delta^{18}O$ is from-6.5 to -2.7 ‰, $\delta^{2}H$ is from -45 to -19 ‰) and is poorly connected to the upstream regions (Fig. 1). The sites RD11 and R11 are estuarine sites, whose $\delta^{18}O$ values are similar to those of the Day River group (Fig. 2a).

Sources of NO_3^- in the Red River delta

The nitrate concentrations ranged between 0.43±0.08 mg L^{-1} at point R3 and 1.98±0.5 mg L^{-1} at point D6 (Fig. 1, Appendix). In general, [NO_3^-] in the D group sites was higher and more variable than in the other group sites. The $\delta^{15}N\text{-}NO_3^-$ values of the Red River group had a smaller isotopic range (+3.8 to +10.0 ‰) than the Day River group (-3.9 to +14.0 ‰). The Red River group peaked at $\delta^{15}N\text{-}NO_3^-$ values around +7 ‰, whilst the Day River group had two $\delta^{15}N\text{-}NO_3^-$ maxima, around +5 and +9 ‰ (Fig. 2b). Statistical test for variance shows that the variances of two populations, $\delta^{15}N\text{-}NO_3^-$ in the Red River and the Day River group, are significantly different ($p < 0.05$). The $\delta^{18}O$-

234 NO_3^- values in the Red River ranged between -4.8 and +6.7 ‰ with a peak value of -1 ‰. The Day
235 River $\delta^{18}O\text{-}NO_3^-$ values ranged between -7.1 and +29.7 ‰ with a peak value of -1 ‰ (Fig. 2b).
236 Also, the two population variances of $\delta^{18}O\text{-}NO_3^-$ were significantly different in the Red River and
237 Day River group ($p < 0.05$).

238 $\delta^{18}O\text{-}NO_3^-$ values in the Red River delta were mostly <+10 ‰ showing no evidence of influence
239 from atmospheric NO_3^- or synthetic NO_3^- fertilizers (Kendall, 1998). Three of the $\delta^{18}O\text{-}NO_3^-$
240 measurements were higher than +10 ‰ (Fig. 3), indicating possible influence from atmospheric
241 NO_3^- and/or NO_3^- synthetic fertilizers. However, these values can result from secondary biological
242 processes that alter the original isotope values (see later) – these values occurred at specific sites
243 and times where river water was severely impacted by domestic wastewater.

244 Using a combined $\delta^{15}N\text{-}NO_3^-$ and $\delta^{18}O\text{-}NO_3^-$ cross plot (following (Kendall, 1998)), we identified
245 three NO_3^- sources in this system; 1) soil leachate, 2) manure and septic waste, and 3) NH_4^+
246 fertilizer leaching. The histogram of $\delta^{15}N\text{-}NO_3^-$ (Fig. 2b) and the bivariate plot (Fig. 3) indicate that
247 NO_3^- in the Red River group is derived mainly from soil. The data also overlap with manure/septic
248 waste NO_3^- sources, but based on the demographic conditions in the region, the manure/septic
249 waste input is unlikely. However, in the Day River group nitrate originates from various sources,
250 including soil leachate (as with the Red River system) NH_4^+ fertilizers, manure and septic waste
251 (Fig.3).

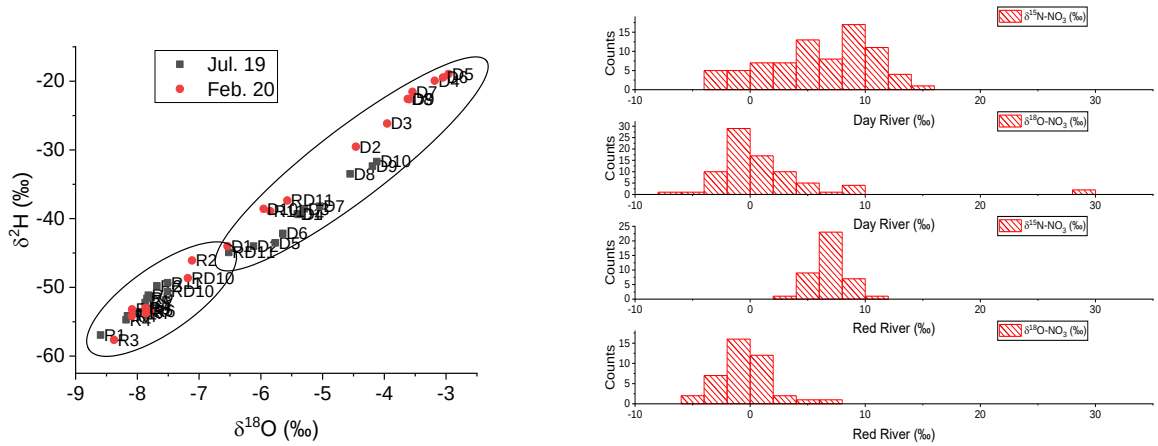

(a) (b)

Fig 2: (a) δ^{18}O-H_2O in rainy (July 2019) and dry (February 2020) seasons. The results show two different water masses in Red River delta; water derived from catchments inside the delta has isotope values higher than ones sourced from upstream mountainous catchments and (b) histogram of δ^{15}N-NO_3^- results in Day River (above) and Red River (below).

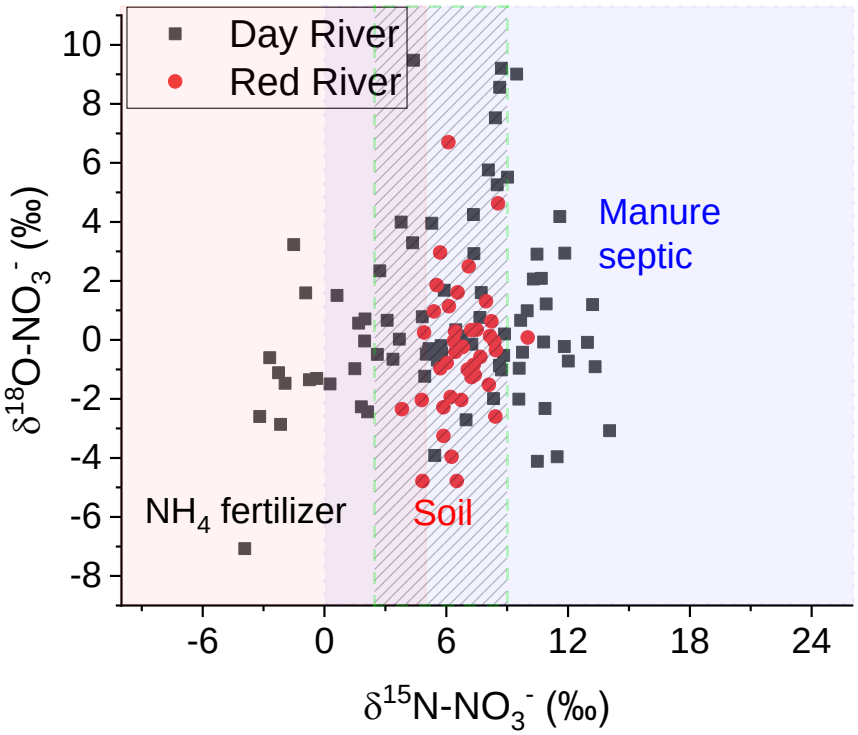

257

258 Fig. 3: Bivariate plot of $\delta^{15}N\text{-}NO_3^-$ vs $\delta^{18}O\text{-}NO_3^-$, implying three sources of NO_3^- in the Red River catchment:
259 NH_4^+ fertilizer, soil leachate, and manure and septic inputs. The Red River group which receives most of
260 its water from upstream sources is dominated by soil-leached NO_3^-, whilst the Day River group which
261 receives water from inside the delta, is dominated by NH_4^+ fertilizers and manure/septic waste.

262 ## Nitrification, denitrification, and biological assimilation

263 The sources of NO_3^- in our catchment, including soil leachates, NH_4^+ fertilizers and sewage/ septic
264 waste are initially reduced nitrogen species, such as ammonium (Trinh, et al., 2012). The NO_3^-
265 derived within the catchment is therefore most likely derived from nitrification. The process of
266 nitrification utilizes surrounding oxygen to oxidize reduced nitrogen compounds to nitrate;

where 2 oxygen atoms are derived from water (H_2O) and 1 oxygen atom from dissolved oxygen (DO) (Snider, et al., 2010).

We investigated the occurrence of nitrification in the catchments by assessing the variability of $\delta^{18}O\text{-}NO_3^-$ as a result of 2/3 of $\delta^{18}O\text{-}H_2O$ and 1/3 of $\delta^{18}O\text{-}O_2$. Our data produced a linear relationship between $\delta^{18}O\text{-}NO_3^-$ and $\delta^{18}O\text{-}H_2O$ expressed by the equation $\delta^{18}O\text{-}NO_3^- = 0.678 \cdot \delta^{18}O\text{-}H_2O + 5.21$ (Fig. 2, appendix), which means that the variability of $\delta^{18}O\text{-}NO_3^-$ is about 2/3 of the $\delta^{18}O\text{-}H_2O$ variability, confirming nitrification as the dominant NO_3^- formation mechanism (Snider, et al., 2010). This finding is consistent with previous studies in the region concluding that nitrate is derived mainly from reduced N species (Trinh, et al., 2007; Trinh, et al., 2012; Luu, et al., 2020). Concomitantly, linear regression results in a $\delta^{18}O\text{-}O_2$ value centering around +15.64±3.94 ‰ (Fig. 2 appendix). Therefore, in order to eliminate the effect of the $\delta^{18}O\text{-}H_2O$ variability/seasonality on the $\delta^{18}O\text{-}NO_3^-$ variability, we normalized $\delta^{18}O\text{-}NO_3^-$ to the associated water $\delta^{18}O\text{-}H_2O$. The normalized $\delta^{18}O\text{-}NO_3^-$ (denoted as $\delta^{18}O\text{-}NO_3^{-}{}_{,H_2O}$) calculation is based on $\delta^{18}O\text{-}NO_3^-$ and $\delta^{18}O\text{-}H_2O$ data from each sample.

$$\text{Normalized } \delta^{18}O\text{-}NO_3^{-}{}_{,H_2O} = \text{Analyzed } \delta^{18}O\text{-}NO_3^- - 2/3 \cdot \delta^{18}O\text{-}H_2O.$$

The normalized $\delta^{18}O\text{-}NO_3^{-}{}_{,H_2O}$ can then be used to assess the relationship between $\delta^{18}O\text{-}NO_3^-$ and NO_3^- concentration, removing variability derived from changing $\delta^{18}O\text{-}H_2O$ (Fig. 4c and d). It should be noted that by this calculation, the normalized $\delta^{18}O\text{-}NO_3^{-}{}_{,H_2O}$ is not referenced to VSMOW but to the local water isotope composition at the time of sampling, thus eliminating the effect of water isotope composition variability.

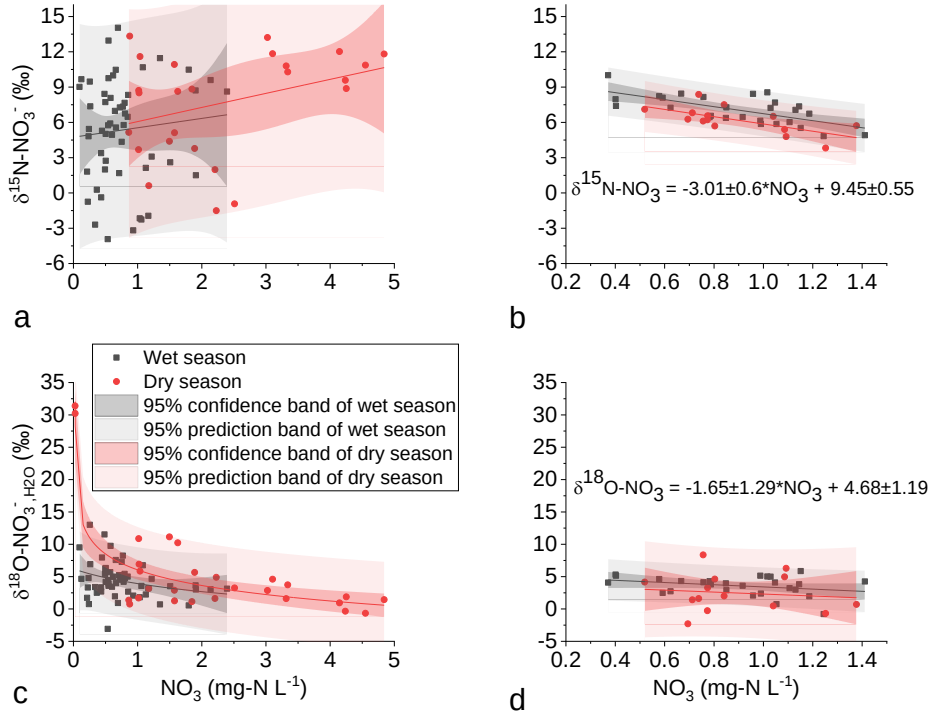

Fig. 4: Nitrate isotopes including $\delta^{15}N\text{-}NO_3^-$ versus $[NO_3^-]$ in (a) the Day River group and (b) the Red River group, and $\delta^{18}O\text{-}NO_{3,H2O}^-$ versus $[NO_3^-]$ in (c) the Day River group, and (d) the Red River group. The data show a logarithmic relationship between the $\delta^{18}O\text{-}NO_{3,H2O}^-$ and $[NO_3^-]$ ($p < 0.05$) and no relationship between $\delta^{15}N\text{-}NO_3^-$ and $[NO_3^-]$ ($p > 0.05$) in the Day River. In the Red River there is a linear relationship between isotopic values and $[NO_3^-]$ ($p < 0.05$) and no significant relationship between $\delta^{15}N\text{-}NO_3^-$ and $[NO_3^-]$. Note that the dry season is from December to May and wet season is from June to November. Dark and light bands indicate respectively 95 % confidence and 95 % prediction of the relationship.

Fig. 4 represents two different scenarios of the dominant processes governing the NO_3^- cycling in the catchment. In the Day River (Fig. 4c), denitrification occurs in some sites during the dry season, serving to decrease NO_3^- concentrations (undetectable in some samples). The remaining

300 NO_3^- pool in these samples is characterized by elevated $\delta^{18}O\text{-}NO_3^-$. In general, denitrification is
301 known to fractionate the NO_3^- pool, resulting in heavier isotope values within the residual NO_3^-
302 (Kendall, 1998). This process occurs only in anoxic environments, where microbial activities rely
303 on NO_3^- as the primary oxygen source. Our data suggest that within the Day River, nitrification
304 and denitrification are both occurring. In the upstream of the shallow Day River, especially during
305 the dry season, water is predominantly urban wastewater with high BOD and concentrated NH_4^+
306 (Trinh, et al., 2007) and the river bed has a high sediment oxygen demand (SOD) (Trinh, et al.,
307 2012). Therefore DO is quickly consumed by biodegradation and slowly replenished by
308 atmospheric oxygen due to slow hydrodynamic condition in the deltaic rivers. This means that
309 the remaining DO is enriched in ^{18}O (Quay, et al., 1995; Piatka, et al., 2022). Next, nitrification in
310 the NH_4^+ concentrated water (Trinh, et al., 2007) utilises the remaining DO within the hypoxic
311 environment (Fig. 1, appendix) to form NO_3^- with extremely high $\delta^{18}O\text{-}NO_3^-$. The newly formed
312 NO_3^- is then diffused and quickly denitrified near the river bottom or in the sediment (Trinh, et
313 al., 2012) reducing the concentration of NO_3^- and enriching the isotopic composition of any that
314 remains. In the Day River group, during the dry season, $\delta^{18}O\text{-}NO_3^-$ is a logarithmic function of
315 $[NO_3^-]$ (Fig. 4c). Such elevated $\delta^{18}O\text{-}NO_3^-$ values where NO_3^- is scarce indicates a combination of
316 nitrification, denitrification, and biological degradation taking place in hypoxic water. During the
317 rainy season hypoxia is less common than during dry season because of rainwater dilution and
318 stronger stream hydrodynamics, and so denitrification cannot occur, as reflected in the weaker
319 relationship between isotopic composition and $[NO_3^-]$ (Fig. 4c). Our explanation for the
320 insignificant and weak positive correlation between $\delta^{15}N\text{-}NO_3^-$ and NO_3^- in the Day River group
321 (Fig. 4a) is that the Day River NO_3^- is dominated by 2 different sources which have different

concentration vs $\delta^{15}N$ relationships; the NH_4^+ fertilizer source characterized by low concentrations of N species and depleted $\delta^{15}N$ and the domestic wastewater source characterized by high concentration of N species and elevated $\delta^{15}N$ (Kendall, 1998). The mixing ratio between the 2 sources controls the variability of $[NO_3^-]$ and $\delta^{15}N\text{-}NO_3^-$, lessening the effect of biogeochemical processes on the $\delta^{15}N\text{-}NO_3^-$ vs NO_3^- relationship.

Within the Red River group we identified no similar evidence of denitrification (Fig. 4d) and no impact of urban waste (Fig. 4b). Nitrate within the Red River group appears to be predominantly derived from soil leaching and where possible nitrification and/or biological assimilation has occurred this has taken place within aerobic waters. The $\delta^{18}O\text{-}NO_3^-$ results therefore clearly indicate different processes occurring within the two systems. As nitrate within the Red River group is predominantly derived from one source which is different from the Day River group, it is easier to interpret the variability of N isotopes in relation to O isotopes as well as to $[NO_3^-]$. The advantage is that $\delta^{15}N\text{-}NO_3^-$ helps to identify the sources independently from water flow, whereas NO_3^- concentrations are diluted in rainy conditions and concentrated in dry periods (Matiatos, et al., 2021). For the Red River group, $\delta^{15}N\text{-}NO_3^-$ isotopic values tended to decrease with higher $[NO_3^-]$. The negative linear correlation between both $\delta^{18}O\text{-}NO_3^-$ and $\delta^{15}N\text{-}NO_3^-$ versus $[NO_3^-]$ (Fig. 4b, d) can be explained due to biological assimilation of N which takes place within the system. Under an assimilation scenario, $[NO_3^-]$ decreases in water and the NO_3^- isotopic signals increases due to preferential uptake of the lighter isotopes.

Overall, the discussion above highlights the complexity of the NO_3^- sources and isotopic response, especially within the Day River group, as the wide range of NO_3^- sources have variable

concentrations and different isotopic signals. The Red River group therefore is simpler, where NO_3^- is mainly derived from upstream soil (Fig. 3). The negative relationship between NO_3^- and its isotopic signals (Fig. 4b and d) might signal biological assimilation (denitrification is unlikely in the aerobic waters of the Red River group, Fig. 1 Appendix). The NO_3^- uptake rate in connection with the NO_3^- isotope enrichment can be calculated from these linear relationships (Fig. 4b and d).

$\delta^{15}N\text{-}NO_3^-$ /normalized $\delta^{18}O\text{-}NO_{3^-,H_2O}$ = 3.01±0.60/1.65±1.29 = 1.82±1.47

This slope of $\delta^{15}N\text{-}NO_3^-$ /normalized $\delta^{18}O\text{-}NO_{3^-,H_2O}$ is within the literature range of nitrate removal reported elsewhere (Lutz, et al., 2020). To calculate the enrichment margin of isotopes due to biological assimilation we can simplify the system by assuming that in the upstream mountain catchment where water is less polluted (primary productivity and respiration are low), $\delta^{18}O\text{-}O_2$ is equilibrated with $\delta^{18}O$ of atmospheric oxygen ($\delta^{18}O\text{-}O_2$ = +23.5 ‰). Then we calculated $\delta^{18}O\text{-}NO_3^-$ as a combination of 2 oxygen atoms from water and 1 atom from DO (Snider, et al., 2010). Next, we compared this calculated $\delta^{18}O\text{-}NO_3^-$ with the analyzed $\delta^{18}O\text{-}NO_3^-$, expecting that the calculated $\delta^{18}O\text{-}NO_3^-$ is lower than the analyzed $\delta^{18}O\text{-}NO_3^-$ to give the $\delta^{18}O\text{-}NO_3^-$ enrichment margin. Then the $\delta^{15}N\text{-}NO_3^-$ enrichment margin was calculated based on Equation 2.

For a simple scenario, we used the mean values of the Red River group data to assess whether or not there is an isotopic enrichment of NO_3^- within the Red River group (the mean±SD of $\delta^{18}O\text{-}H_2O$ = -7.84±1.00 ‰ and the mean±SD of normalized $\delta^{18}O\text{-}NO_{3^-,H_2O}$ = +3.21±2.13 ‰).

=> The calculated $\delta^{18}O\text{-}NO_3^-$ = (2*$\delta^{18}O\text{-}H_2O$ + $\delta^{18}O\text{-}O_2$)/3 = (2*(-7.84±1.00) +23.5)/3 = 2.61±0.67 ‰.

364 => The $\delta^{18}O\text{-}NO_3^-$ enrichment margin = normalized $\delta^{18}O\text{-}NO_{3,H_2O}^-$ - calculated $\delta^{18}O\text{-}NO_3^-$ =

365 3.21±2.13 – 2.61±0.67 = 0.6±2.23 ‰.

366 => The $\delta^{15}N\text{-}NO_3^-$ enrichment margin (Equation 2) is 0.6±2.23*1.82±1.47 = 1.09±4.15 ‰.

367 Based on Fig. 4b, the isotope enrichment is converted to the NO_3^- uptake as 1.09±4.15/3.01±0.60

368 = 0.36±1.37 (mg-N L^{-1}).

369 In order to evaluate the validity of the isotope enrichment margin calculated here, we estimated

370 the range of the NO_3^- uptake rate based on the growth of autotrophs in the water column and

371 compared the NO_3^- uptake obtained by the two approaches. According to (Trinh, et al., 2006),

372 autotrophic growth can be calculated as:

373 $$Growth_{Auto} = k_{growth.max}\frac{NO_3}{K + NO_3}k_{Light}e^{(1-k_{Light})}Auto$$

374 Where *K* = 0.1 (mg-N L^{-1}), k_{Light}, the irradiation coefficient, ranges from 0 to 1, and *Auto* =

375 autotroph biomass (mg-C L^{-1}). We estimated autotroph biomass (*Auto*) from the chlorophyll a

376 (*Chl a*) concentration: *Auto* (mg-C L^{-1}) = 40*Chl a (mg L^{-1}) (Jakobsen & Markager, 2016). We used

377 the Redfield ratio (C:N:P = 106:16:1) to calculate the NO_3^- assimilation due to autotrophic growth.

378 The above equation is changed to:

379 $$Uptake_{NO_3} = k_{growth.max}\frac{NO_3}{K + NO_3}k_{Light}e^{(1-k_{Light})}Chl\ a\frac{40 \times 16 \times 14}{106 \times 12}$$

380 We used *Chl a* = 30 (μg L^{-1}) in the Day River (Trinh, et al., 2007) and $k_{growth.max}$ = 2.0 (d^{-1}) (Trinh,

381 et al., 2006) to come to the NO_3^- uptake rate between 0 and 0.42 (mg-N L^{-1} d^{-1}). The flow velocity

382 of Red River is around 1 m s^{-1} (Sai, et al., 2020). Water reaching the main stream (Red River length

383 is over 1000 km) would need less than 10 days to reach the Red River delta. Thus, the uptake
384 margin calculated by this approach is between 0 and 4.2 mg-N L^{-1}. Comparison between the
385 uptake margin calculated from isotopic data and the uptake rate calculated from Trinh et al.
386 (2006) shows that the isotopically calculated uptake margin is within the range of autotroph
387 growth uptake – the difference is within an order of magnitude. The validity of calculated values
388 here, thus confirms the possibility of denitrification and/or biological assimilation of NO_3^- inside
389 the water column of the Red River system using our isotopic data.

390 ## Estimation of $\delta^{18}O$-O_2 to assess metabolic state

391 Dissolved oxygen (DO) is a crucial component for aquatic life (Odum, 1956; Stumm & Morgan,
392 1996). DO concentration is controlled to a large extent by air–water gas exchange (G), aquatic
393 primary production (P) and consumption rates through community respiration (R). The balance
394 between production and consumption is driven by nutrient availability, temperature, light,
395 substrate availability, and other environmental conditions (Odum, 1956; Stumm & Morgan,
396 1996). Traditionally, aquatic metabolic state has been reported as the P:R ratio (Wilcock, et al.,
397 (1998) ; Wetzel, 2001). Ecosystem metabolic balance, whether predominantly heterotrophic (P:R
398 < 1) or autotrophic (P:R > 1), is often indicated by the degree of O_2 saturation. In a P:R equilibrium
399 and steady state aquatic ecosystem, the amount of oxygen consumed by respiration is equal to
400 the one produced from primary production and DO is sourced from atmospheric exchange only.
401 In a dynamic/unsteady state ecosystem where gas exchange might be too slow or too fast
402 compared to the net P+R sources, DO could be saturated or undersaturated relative to the
403 atmosphere, but it does not reflect if P is equal to or higher than R (Venkiteswaran, et al., 2007).
404 In other words, the saturation level of DO may not truly reflect the metabolic state (autotrophic

405 or heterotrophic) of aquatic ecosystems. Here, we aim to use the isotopic value of DO as an
406 indicator of metabolic state within our river ecosystems (Venkiteswaran, et al., 2007).

407 The principle behind using the stable isotope composition of DO to assess the ecosystem
408 metabolic state is that respiration and biodegradation processes drive higher $\delta^{18}O\text{-}O_2$ values
409 while photosynthesis would lower $\delta^{18}O\text{-}O_2$ (Quay, et al., 1995; Piatka, et al., 2022). If one process
410 dominates, this is reflected by clearly higher or lower isotope values. Aerobic respiration by
411 microorganisms (protozoa, bacteria, and phytoplankton) causes a significant organism-level O-
412 isotope fractionation, a result of the preferential consumption of the lighter isotopologue, $^{16}O_2$.
413 Hence, respiration leads to a detectable increase in the ^{18}O:^{16}O ratio of O_2 in the residual water
414 pool (Parker, et al., 2005; Lehmann, et al., 2009). Conversely, O_2 generated during aquatic
415 primary production is derived from oxidizing ambient water molecules. This process does not
416 cause significant O_2 isotope fractionation and adds dissolved O_2 to the aquatic ecosystem with
417 $\delta^{18}O$ values identical to that of the water (Stevens, et al., 1975; Helman, et al., 2005). The $\delta^{18}O\text{-}$
418 O_2 of photosynthetic O_2 (derived from surrounding water) added to the dissolved O_2 pool is
419 always more depleted in ^{18}O (range between -11.2 and -2.7 ‰ in the Red River delta water, Fig.
420 2a) than atmospheric O_2 (+23.5 ‰). Given the large difference between the $\delta^{18}O$ of atmospheric
421 O_2 and water oxygen ($\delta^{18}O\text{-}H_2O$), $\delta^{18}O\text{-}O_2$ assays are well suited to detect the addition of small
422 amounts of photosynthetic O_2 to aquatic ecosystems.

423 Since our study did not directly analyze the isotopic composition of DO, we proposed a method
424 to estimate $\delta^{18}O\text{-}O_2$ with the use of $\delta^{18}O\text{-}H_2O$ and $\delta^{18}O\text{-}NO_3^-$, assuming that NO_3^- is produced from
425 nitrification of reduced N species, consisting of 2 oxygen atoms derived from surrounding water

molecules and 1 oxygen atom from dissolved oxygen (discussed previously) and that no large fractionations of nitrate isotope composition (e.g. from denitrification) take place in this shallow river system, as there is no isotopic evidence for this apart from in the Day River system in the dry season and slight enrichment in the Red River system as concluded above (the $\delta^{18}O\text{-}NO_3^-$ enrichment margin = 0.6±2.23 ‰). One advantage of our method is that because nitrification takes place both day and night and the residence time of NO_3^- is much longer than of O_2 gas in water, the NO_3^- oxygen isotopes should reflect the whole transient diel O_2 isotopic pattern; not simply the daytime (when oxygen is produced in excess over dark respiration) or the night (when production of oxygen through primary productivity does not take place) (Venkiteswaran, et al., 2007).

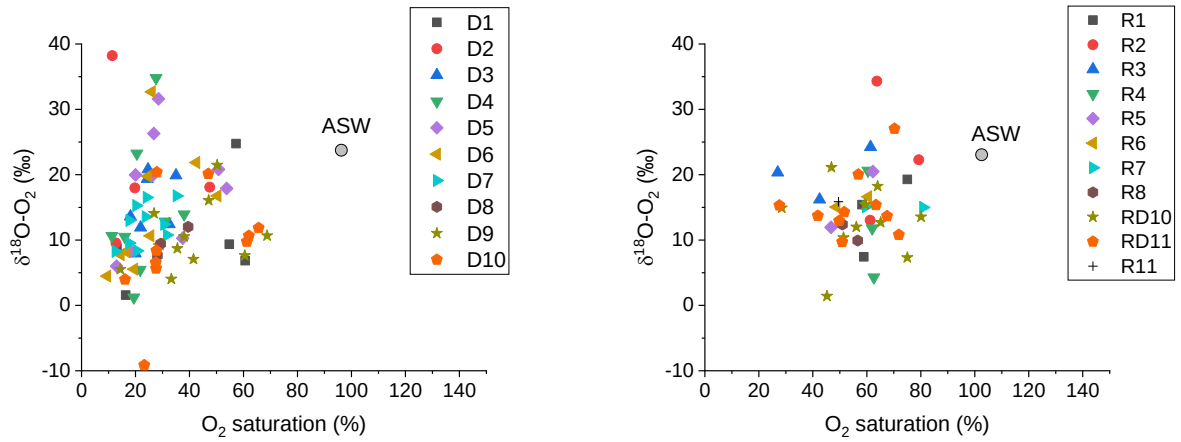

Fig. 5: $\delta^{18}O\text{-}O_2$ estimated from $\delta^{18}O\text{-}H_2O$ and $\delta^{18}O\text{-}NO_3^-$ versus O_2 saturation level (%) for the Day River group (a) and the Red River group (b). ASW = air saturated water at equilibrium.

The majority of the calculated $\delta^{18}O\text{-}O_2$ in both river groups (mean $\delta^{18}O\text{-}O_2$ = +15.64±3.94 ‰) is below the equilibrium value for air saturated water +23.5 ‰ (Fig. 5) implying a dominance of autotrophic production in the water column, especially at agricultural sites (D7-10, R6-8, RD10).

441 There is a strong variability of $\delta^{18}O\text{-}O_2$ at sites close to the urban area (D1-6, R4-5), indicating a
442 high seasonality of metabolic state there. The results imply that a large fraction of DO is
443 generated from in stream photosynthesis. At the same time however, DO is lower than saturation
444 throughout, indicating a stronger cumulative respiration (oxygen consumption) rate than primary
445 production, plus atmospheric exchange (oxygen productivity). Only at site R2 (Lo tributary) are
446 $\delta^{18}O\text{-}H_2O$ and DO close to atmospheric levels, which we explain by the reduction of all biological
447 activities (P and R) within this tributary (Lo River). The catchment of the Lo tributary is more
448 dominated by limestone bedrock than the other catchments and its relatively unpolluted water
449 could be a reason for this low primary productivity (Moon, et al., 2007). Our explanation for the
450 fact that water in the Red River delta is consistently well below O_2 saturation (5–80 %, Fig. 5) is
451 that in tropical, lowland, delta river systems that are heavily impacted by anthropogenic inputs,
452 sediments and anthropogenically impacted water inflows may play an important role (Trinh, et
453 al., 2007; Trinh, et al., 2012), consuming a large portion of DO without causing large isotope
454 fractionation. Thus, the water column tends to be autotrophic but the whole river system
455 including sediment, and especially when merged with anoxic wastewater fluxes, is low in DO.

456 The mean estimated $\delta^{18}O\text{-}O_2$ of Red River and Day River groups are similar (mean±SD =
457 +15.16±5.9 and +15.66±15.9 ‰, respectively). If we assume that the ratio of primary
458 production/respiration rates (2 processes that fractionate $\delta^{18}O\text{-}O_2$) are identical between the two
459 river groups and knowing the measured DO % (mean±SD of DO in 2 river groups are 57.39±12.87
460 and 29.04±15.34 %, respectively), then we can define the oxygen consumption in the river
461 system. A system with significant biological respiration (BOD) will have clearly fractionated
462 oxygen isotopic composition of DO, whereas a system with large chemical oxygen demand (COD,

SOD) and anoxic wastewater inputs will not fractionate the isotopic composition of oxygen. With these differential isotopic effects on DO, we can conclude that the oxygen demand in the Day River group is high relative to the Red River group; as dissolved oxygen concentration is lower in the Day River group than in Red River group, while isotopic composition is the same between the two groups. The explanation for the lower DO level (higher oxygen demand) in the Day than the Red River groups is apparently anthropogenic and exacerbated by stagnant waters (Salgado, et al., 2022). Urbanization and industrialization in Day River catchment have caused environmental disaster in the ecosystem (Trinh, et al., 2007; Trinh, et al., 2012). Biological activities, on the other hand, are indifferent between the two rivers.

Spatial-temporal variability of N sources

The above discussion leads to the conclusion that there are 3 main sources of NO_3^- in the Red River delta: the upstream/soil source, the agricultural NH_4^+-fertilizer source, and the urban source. The partitioning among these 3 sources drives the measured $\delta^{15}N\text{-}NO_3^-$ composition in the river waters. Deviation from the 3-source partition value comes only from isotope fractionation associated with denitrification and biological assimilation. On the other hand, $\delta^{18}O\text{-}NO_3^-$ variability in the Red River delta water is controlled by $\delta^{18}O\text{-}O_2$ and $\delta^{18}O\text{-}H_2O$, which are highly variable, especially in the Day River where $\delta^{18}O\text{-}O_2$ is a function of metabolism (high in heterotrophic and low in autotrophic).

Spatial variability:

Averages of the NO_3^- fractions for different sites show that soil NO_3^- is the dominant source of NO_3^- within the entire catchment, with the only exceptions being sites D1, D9 and D10 (Fig 6 and

484 Table 3). Site R2 comes from an unpolluted upland water source, derived from a mountain region
485 and not flowing through urban or agricultural centers, this site shows almost 100 % soil - derived
486 NO_3^-. A clear trend emerges along the catchment with soil derived NO_3^- accounting for nearly 80
487 % in upstream sites and gradually reducing to around 60 % when at the coast (Table 3). This
488 decrease is associated with the additional loading for NO_3^- from urban and agricultural sources.

489

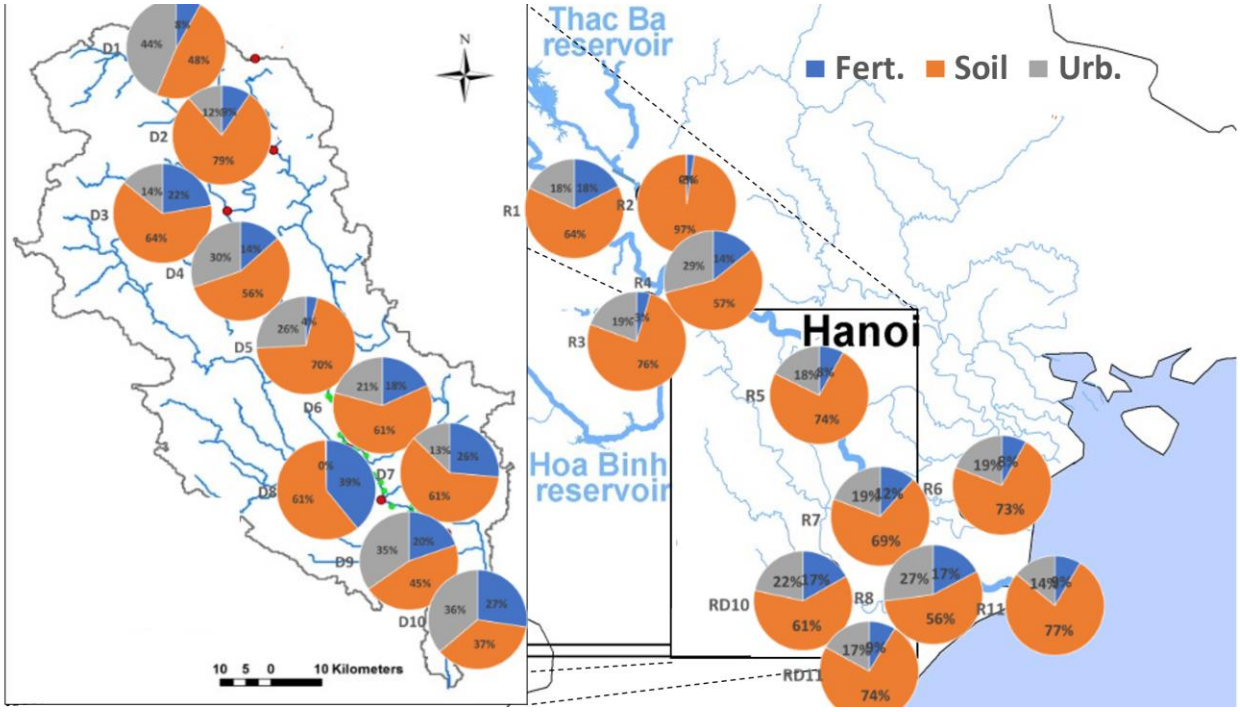

490

491 Fig. 6: Mean values of the NO_3^- fractions (%) at different monitoring sites

492 The middle of the delta is characterised by a step change in NO_3^- derived from manure and septic
493 tank contributions, associated with the urbanization of the catchment and poor waste
494 management strategies (Table 3). The highest loading of urban wastewater is observed at sites
495 D1-D6, D9 and D10 (Fig 6), all located near or downstream of major urban settlements. On
496 average, fertilizer load increases slightly in the lower regions of delta (Table 3) characterised by

497 intensive agriculture, mostly rice farming, with sites D7-D10 having >20 % NO_3^- derived from
498 agricultural sources (Fig 6). Rice growth practices require large volumes of water to create
499 submerged paddy fields, leading to the leaching of fertilisers back into the main river system.
500
501 Table 3: Average fractions of NO_3^- sources in different zones in the Red River delta. Sites are grouped into
502 mountain upstream sites (R1-3, D8), urban sites (D1-6), paddy field/agricultural dominated sites (D7, 9,
503 10, RD10, 11, R4-8, 11) as clearly sketched in Fig. 1.

Zones	Fertilizer (mean±SE)	Manure/septic (mean±SE)	Soil derived (mean±SE)
Mountain (upper)	0.12±0.21	0.10±0.17	0.78±0.27
Urban (middle)	0.13±0.18	0.25±0.29	0.62±0.21
Agricultural (lower)	0.18±0.18	0.24±0.23	0.58±0.25

504
505 The soil fraction is the dominant source in all zones, significantly higher than a combination of
506 NH_4^+ fertilizer washout and sewage/septic input (anthropogenic sources) (paired t-tests, $p <$
507 0.05). However, further comparison indicates an increasing contribution of anthropogenic
508 activities to NO_3^- in river water. In the urban zone, the manure/septic input is significantly higher
509 than fertilizer washout, while elsewhere the contribution of fertilizer and manure/septic sources
510 is statistically similar. The fraction of NH_4^+ fertilizer was not significantly different between zones
511 but there is a trend towards higher proportions in the agricultural zone relative to the urban and
512 mountain zones (t-tests, $p > 0.05$). The fraction of manure/septic input was significantly lower in
513 mountain zone than in the 2 other zones. Together with the fact that the fraction of soil leaching
514 is significantly higher in the mountain zone than in agricultural zone, we can infer higher
515 anthropogenic impact in the downstream region, especially in urban areas. The spatial
516 assessment of NO_3^- loading into the catchment highlights a trend of increasing pollution from

517 urban and agricultural sources, especially within the Day River. As discussed above however, this
518 trend is also impacted by seasonal variations in NO_3^- additions during rainy vs dry seasons.

519 Seasonality:

520 There are clear trends in NO_3^- loading within the mid and lower sections of the Day River system.
521 Figure 7 groups and shows a seasonal assessment of the D6, 7, 9, 10 and RD10, 11 sites from the
522 Day River, which are shown from Figure 6 to be the most impacted by anthropogenic activities in
523 either the Day or Red River catchments. Our results indicate a high manure and septic NO_3^- signal
524 during dry periods (Nov-April) and a low signal with far higher contributions from soil sources in
525 the rainy period (July-Sept). Two outliers from this overall trend can be seen, the first, in February
526 and the second in November. February is a critical period for watering the spring rice crop in the
527 Red River delta. As this is a dry period within the delta, irrigation water is provided from upstream
528 (Fig. 7), resulting in a lower observed urban load and higher soil contributions in February.

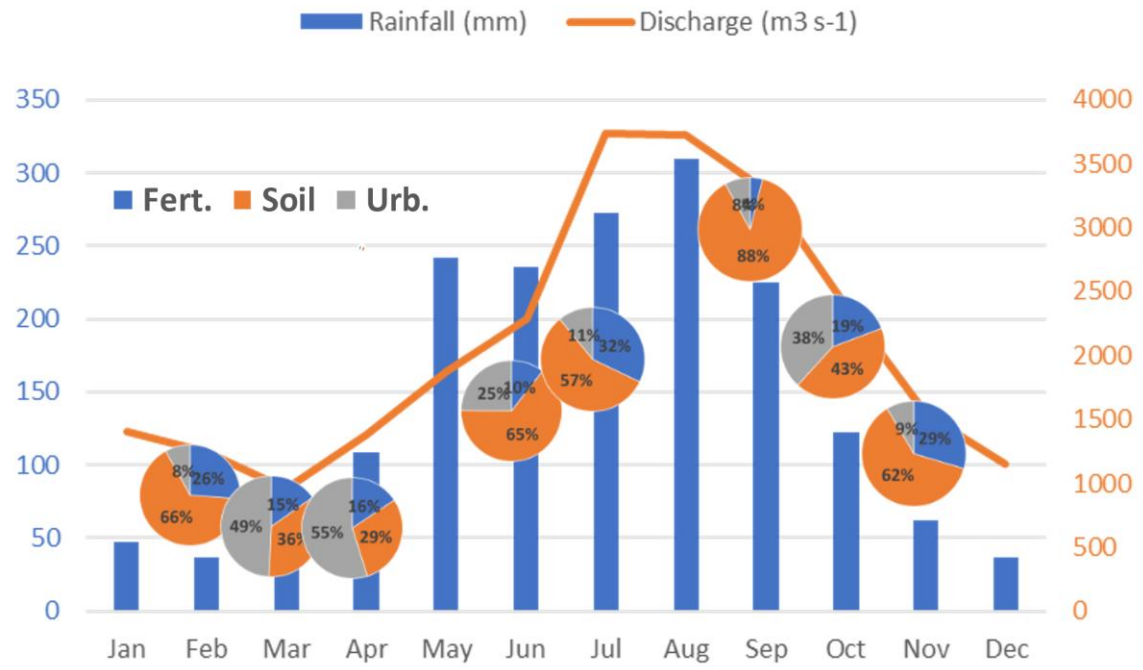

Fig. 7: Seasonality of the NO_3^- fractions in the middle-lower sections of Day River group (D6,7, 9, 10, RD10, 11) where water should practically suffer more from anthropogenic impacts than the upstream and Red River group sites. Rainfall is recorded for the 1991-2021 period. Discharge is recorded for 2017-2020 period. Both records are in Hanoi (R5). It should be noted that most of our sampling were taken place the first week of the month. It is therefore logical to associate the isotopic data with the hydro-meteorological data of the precedent months.

The unexpectedly high fraction of soil-leached NO_3^- in November is explained by the fact that we have only one data point in November 2018 when upstream discharge was particularly high (the discharge is 2440 and 1950 $m^3 s^{-1}$ in Oct. and Nov. 2018, respectively, much higher than the mean 2017-2020 records, Fig. 7). This extreme discharge is most probably the reason for the higher than expected contribution of soil NO_3^-, which is washed in from further up the catchment or eroded from banks whilst in flood; resulting in a relatively reduced contribution of urban NO_3^-.

Unlike soil and urban contributions, fertilizer leaching varies monthly within the catchment, reflecting agricultural practices in the region (Luu, et al., 2020). Traditionally, there are two cropping seasons in the Red River delta (November-May and May-November crops). Each crop requires several rounds of fertilizer application annually. Therefore, we observe less clear seasonality in fertilizer derived NO_3^- as this is solely an anthropogenically-driven pollution source. However, relatively speaking, the magnitude of fertilizer leaching is less than that of manure and septic waste NO_3^- (Table 3 and Fig. 7). This implies a strong impact of urbanization on NO_3^- pollution, in particular, and water quality, in general.

Conclusions

The Red River delta is home to tens of millions of people who rely on the catchment as their primary water resource for industry and agriculture. This critical resource is rapidly becoming impacted by anthropogenic activities and nitrate pollution is thought to be negatively influencing the metabolic state of much of the Red River delta.

This study highlights the advantages of using stable isotopes for tracing NO_3^- sources and identifying the biogeochemical processes in aquatic ecosystems responsible for transformations of N. Isotopic variability of water and NO_3^- highlights intense biogeochemical activity and complex anthropogenic inputs (both agriculture and urbanization) within the Red and Day River systems. Nitrate in the Red River delta is derived from soil leaching and anthropogenic inputs (NH_4^+ fertilizer application and domestic waste discharge).

Urbanization contributes a large fraction of total NO_3^-; sometimes higher than 50 % of total load, as seen in the middle section of the Day River during dry season. High inputs of domestic waste

result in heterotrophic conditions (Salgado, et al., 2022); low dissolved oxygen, as clearly indicated by enriched $\delta^{18}O\text{-}NO_3^-$.

This research underlines a broader, and rather pressing, concern — despite being autotrophic in nature, high inputs of degradable organic matter have compromised the river's oxygen levels. This oxygen undersaturation coupled with high NO_3^- loads poses a dire threat to water quality and, by extension, to the health and well-being of millions who rely on this river system.

Our approach to assess the aquatic metabolism state using nitrate and water isotopes is an indirect proxy and remains to be tested with an actual investigation of dissolved oxygen stable isotopes in future.

Based on this work we can propose a simple mitigation strategy to help manage NO_3^- contributions to the Red River catchment when it is most vulnerable to NO_3^- pollution. This would target the dry season and would involve the pumping of water from the Red River's mainstream into the Day River's upstream section during dry periods. This would have the impact of diluting the Day River with less polluted waters and elevating to some extent the impact of urban pollutants. As the dry season is also a period of maximum irrigation within the Day River, this would also enable more water to be pumped into paddy fields in order to fertilize the spring crop. This re-distribution of water would in fact be re-establishing natural linkages between the river systems. Only since French colonization (100 years ago) was a dam built to prevent inundation into Hanoi (Trinh, et al., 2007), disconnecting the Red River from the upper Day River. A managed reestablishment of this connection appears a relatively straightforward strategy for mitigation of NO_3^- pollution and ecosystem damage.

Acknowledgements

The fieldwork and laboratory analyses were consecutively conducted within the frameworks of the IAEA-CRP F32007, the NERC-NAFOSTED NE/P014577/1, the UKRI GCRF Living Deltas Hub NE/S008926/1 and the MOST-OeAD NĐT/AT/22/27 research projects.

References

Chang, C. C. et al., 1999. A method for nitrate collection for δ15N and δ18O analysis from waters with low nitrate concentrations. *Canadian Journal of Fisheries and Aquatic Sciences,* 56(10), pp. 1856-1864.

Clesceri, L. S., Greenberg, A. E. & Eaton, A. D., 1998. *Standard Methods for the Examination of Water and Wastewater, 20th Edition.* s.l.:APHA American Public Health Association.

Coplen, T. B. & Wassenaar, L. I., 2015. LIMS for Lasers 2015 for achieving long-term accuracy and precision of δ2H, δ17O, and δ18O of waters using laser absorption spectrometry. *Rapid Communications in Mass Spectrometry,* Volume 29, pp. 2122-2130.

Denk, T. R. et al., 2017. The nitrogen cycle: A review of isotope effects and isotope modeling. *Soil Biology & Biochemistry,* Volume 105, pp. 121-137.

Helman, Y. et al., 2005. Fractionation of the three stable oxygen isotopes by oxygen-producing and oxygen-consuming reactions in photosynthetic organisms. *Plant Physiol ,* Volume 138, p. 2292–2298. doi:10.1104/pp.105.063768.

605 Jakobsen, H. H. & Markager, S., 2016. Carbon-to-chlorophyll ratio for phytoplankton in temperate
606 coastal waters: Seasonal patterns and relationship to nutrients. *Limnology and oceanography,* p.
607 doi.org/10.1002/lno.10338.

608 Kendall, C., 1998. Chapter 16 - Tracing Nitrogen Sources and Cycling in Catchments. In: C.
609 KENDALL & J. J. McDONNELL, eds. *Isotope Tracers in Catchment Hydrology.* Amsterdam: Elsevier,
610 pp. 519-576.

611 Lehmann, M. F. et al., 2009. Aerobic respiration and hypoxia in the Lower St. Lawrence Estuary:
612 Stable isotope ratios of dissolved oxygen constrain oxygen sink partitioning. *Limnology and*
613 *oceanography,* 54(6), pp. 2157-2169.

614 Lutz, S. R. et al., 2020. How Important is Denitrification in Riparian Zones? Combining End-
615 Member Mixing and Isotope Modeling to Quantify Nitrate Removal from Riparian Groundwater.
616 *water resource research,* Volume 56, p. e2019WR025528.

617 Luu, T. N. M., Do, T. N., Matiatos, I. P. V. N. & Trinh, A. D., 2020. Stable isotopes as an effective
618 tool for N nutrient source identification in a heavily urbanized and agriculturally intensive tropical
619 lowland basin. *Biogeochemistry,* Volume 149, p. 17–35.

620 Marković, T. et al., 2022. Tracking the nitrogen cycle in a vulnerable alluvial system using a multi
621 proxy approach: Case study Varaždin alluvial aquifer, Croatia. *Science of the Total Environment,*
622 853(20), p. 158632.

623 Matiatos, I. et al., 2023. Stable isotopes reveal organic nitrogen pollution and cycling from point
624 and non-point sources in a heavily cultivated (agricultural) Mediterranean river basin. *Science of*
625 *The Total Environment, ,* Volume 901, p. 66455.

626 Matiatos, I., Wassenaar, L. I., Monteiro, L. R. & al, e., 2021. Global patterns of nitrate isotope
627 composition in rivers and adjacent aquifers reveal reactive nitrogen cascading. *Communications*
628 *Earth & Environment,* Volume 2, p. 52.

629 McIlvin, M. R. & Altabet, M. A., 2005. Chemical Conversion of Nitrate and Nitrite to Nitrous Oxide
630 for Nitrogen and Oxygen Isotopic Analysis in Freshwater and Seawater. *Analytical Chemistry,*
631 Volume 77, pp. 5589-5595.

632 Moon, S., Huh, Y., Qin, J. & Nguyen, v. P., 2007. Chemical weathering in the Hong (Red) River
633 basin: Rates of silicate weathering and their controlling factors. *Geochimica et Cosmochimica*
634 *Acta ,* Volume 71, p. 1411–1430.

635 Nguyen, N. L., Do, T. N. & Trinh, A. D., 2021. Application of Water Stable Isotopes for Hydrological
636 Characterization of the Red River (Asia). *Water,* 13(15), pp. 2051-2064.

637 Odum, H., 1956. Primary Production in Flowing Waters. *Limnology and Oceanorgraphy,* Volume
638 1, p. 102–117.

639 Pardo, L. H., Kendall, C., Pett-Ridge, J. & Chang, C. C. Y., 2004. Evaluating the source of
640 streamwater nitrate using d15N and d18O in nitrate in two watersheds in New Hampshire, USA.
641 *Hydrological Processes ,* Volume 18, p. 2699– 2712.

642 Parker, S. R., POULSON, S. R., GAMMONS, C. H. & DEGRANDPRE, M. D., 2005. Biogeochemical
643 controls on diel cycling of stable isotopes of dissolved O2 and dissolved inorganic carbon in the
644 Big Hole River, Montana.. *Environ. Sci. Technol. ,* Volume 39, p. 7134–7140..

645 Piatka, D. R. et al., 2022. Dissolved oxygen isotope modelling refines metabolic state estimates
646 of stream ecosystems with different land use background. *Scientific report,* Volume 12, p. 10204.

647 Quay, P. D. et al., 1995. The 18O:16O of dissolved oxygen in rivers and lakes in the Amazon Basin:
648 Determining the ratio of respiration to photosynthesis rates in freshwaters. *Limnology and*
649 *Oceanography,* Volume 40, pp. 718-729.

650 Roberts, L. et al., 2022. In flux: Annual transport and deposition of suspended heavy metals and
651 trace elements in the urbanised, tropical Red River Delta, Vietnam. *Water Research,* Volume 224
652 , p. 119053.

653 Sai, H. A. et al., 2020. An optimal scenario for the emergency solution to protect Hanoi Capital
654 from the Red River floodwater using Van Coc Lake. *Journal of Flood Risk Management,* 13 (4), p.
655 e12661.

656 Salgado, J. et al., 2022. Urbanization and seasonality strengthens the CO2 capacity of theRed
657 River Delta, Vietnam. *Environ. Res. Lett. ,* Volume 17 , p. 104052.

658 Silva, S. et al., 2000. A new method for collection of nitrate from fresh water and the analysis of
659 nitrogen and oxygen isotope ratios. *Journal of Hydrology,* 228(1–2), p. 22.

660 Snider, D. M., Spoelstra, J., Schiff, S. L. & Venkiteswaran, J. J., 2010. Stable Oxygen Isotope Ratios
661 of Nitrate Produced from Nitrification: 18O-Labeled Water Incubations of Agricultural and
662 Temperate Forest Soils. *Environmental Science & Technology,* 44(14), p. 5358–5364.

663 Steffen, W. et al., 2015. Planetary boundaries: Guiding human development on a changing planet.
664 *Science,* 347(6223), p. 1259855.

665 Stevens, C., Schultz, D., Vanbaalen, C. & P., P., 1975. Oxygen Isotope Fractionation During
666 Photosynthesis in a Blue-Green and a Green- Alga. *Plant Physiol ,* Volume 56, p. 126–129 .

667 Strokal, M. et al., 2016. Alarming nutrient pollution of Chinese rivers as a result of agricultural
668 transitions.. *Environmental Research Letters.,* 11(2), p. 024014..

669 Stumm, W. & Morgan, J., 1996. *Aquatic chemistry.* third edn ed. New York: Wiley–Interscience, .

670 Ta, T. T. et al., 2016. Interpretation of anthropogenic impacts (agriculture and urbanization) on
671 tropical deltaic river network through the spatio-temporal variation of stable (N, O) isotopes of
672 NO−3. *Isotopes in Environmental and Health Studies,* Volume 52, pp. 487-497.

673 Trinh, A. D. et al., 2006. Biochemical modeling of the Nhue River (Hanoi, Vietnam): Practical
674 identifiability analysis and parameter estimation. *Ecological modeling,* 193((3-4)), pp. 182-204.

675 Trinh, A. D., Meysman, F., Rochelle-Newall, E. & Bonnet, M. P., 2012. Quantification of sediment-
676 water interactions in a polluted tropical river through biogeochemical modeling. *Global*
677 *Biogeochemical Cycles,* Volume 26.

678 Trinh, A. D. et al., 2007. Experimental investigation and modelling approach of the impact of
679 urban wastewater on a tropical river; a case study of the Nhue River, Hanoi, Viet Nam. *Journal of*
680 *hydrology,* 334((3–4)), pp. 347-358.

681 Venkiteswaran, J., Boeckx, P. & Gooddy, D., 2019. Towards a global interpretation of dual nitrate
682 isotopes in surface waters. *Journal of Hydrology X ,* Volume 4, p. 100037.

683 Venkiteswaran, J. J., Wassenaar, L. I. & Schiff, S. L., 2007. Dynamics of dissolved oxygen isotopic
684 ratios: a transient model to quantify primary production, community respiration, and air–water
685 exchange in aquatic ecosystems. *Oecologia ,* Volume 153, p. 385–398.

686 Wassenaar, L. I., Coplen, T. B. & Aggarwal, P. K., 2014. Approaches for Achieving Long-Term
687 Accuracy and Precision of δ18O and δ2H for Waters Analyzed using Laser Absorption
688 Spectrometers. *Environmental Science & Technology,* Volume 48, pp. 1123-1131.

689 Wetzel, R., 2001. *Limnology—Lake and River Ecosystems.* San Diego, Calif.: Academic Press.

690 Wilcock, R. et al., (1998) . Characterisation of lowland streams using a single-station diurnal curve
691 analysis model with continuous monitoring data for dissolved oxygen and temperature. *N Z J Mar*
692 *Fresh Res ,* Volume 32, pp. 67-79.

693 Xue, D. et al., 2009. Present limitations and future prospects of stable isotope methods for nitrate
694 source identification in surface- and groundwater. *Water research,* Volume 43, p. 1159–1170.

695 Zeng, L. et al., 2023. Ecosystem deterioration in the middle Yangtze floodplain lakes over the last
696 two centuries: Evidence from sedimentary pigments. *Quaternary Science Reviews,* Volume 302,
697 p. 107954..

698

699 # Appendix

700

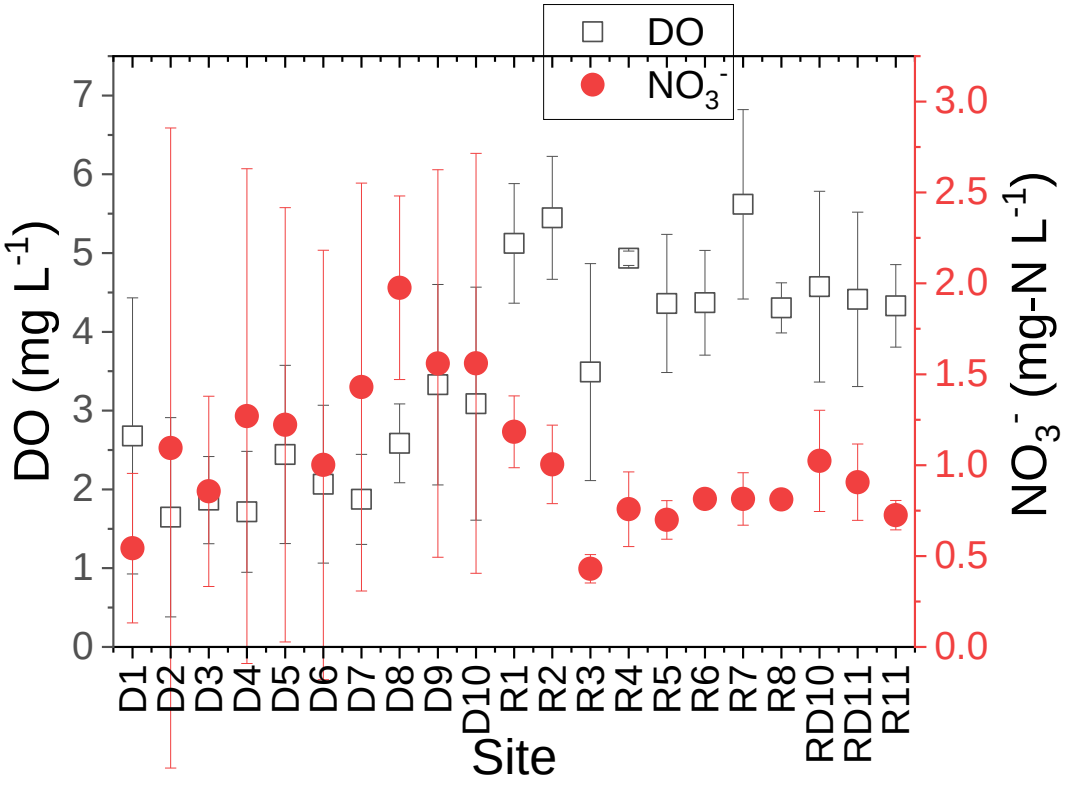

701

702 Fig. 1: Mean ± standard deviation of dissolved oxygen (DO) and nitrate (NO_3^-) concentration in

703 water samples at different monitoring sites.

704

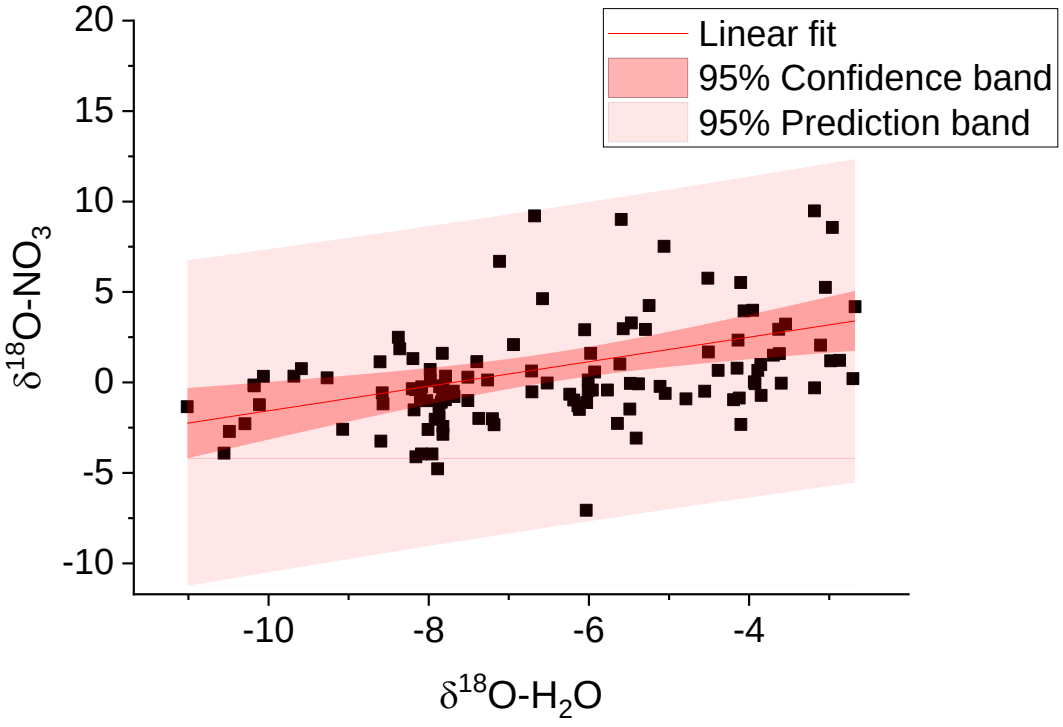

705

706 Fig. 2: $\delta^{18}O\text{-}NO_3^-$ vs $\delta^{18}O\text{-}H_2O$ indicating a positive relationship (p-value = $6.8E^{-4}$ << 0.05) between
707 2 variables in which $\delta^{18}O\text{-}NO_3^-$/ $\delta^{18}O\text{-}H_2O$ is 0.678 (approx. 2:3). According to (Snider, et al., 2010),
708 the intercept of regression line represents approx. 1:3 of the mean of $\delta^{18}O\text{-}O_2$ => the mean ± SD
709 of $\delta^{18}O\text{-}O_2$ in the Red River delta is 15.64±3.94 ‰. This value is lower than the $\delta^{18}O\text{-}O_2$ in
710 equilibrium with atmospheric oxygen (24.2 ‰). Thus, this calculation is another indicator that
711 P>R in the Red River delta although DO level is mostly undersaturated. Another explanation for
712 the low calculated $\delta^{18}O\text{-}O_2$ is that isotopic fractionation of cumulative respiration in the Red River
713 delta is low due to the contributions of such SOD, COD, and anoxic wastewater fluxes which
714 indiscriminately consume heavier and light isotopes.